NISTIR 89-3917

IMPROVED LOW-LEVEL SILICON-AVALANCHE-PHOTODIODE TRANSFER STANDARDS AT 1.064 MICROMETERS

A.L. Rasmussen
P.A. Simpson
A.A. Sanders

National Institute of Standards and Technology
U.S. Department of Commerce
Boulder, Colorado 80303-3328

August 1989

NISTIR 89-3917

IMPROVED LOW-LEVEL SILICON-AVALANCHE-PHOTODIODE TRANSFER STANDARDS AT 1.064 MICROMETERS

A.L. Rasmussen
P.A. Simpson
A.A. Sanders

Electromagnetic Technology Division
Center for Electronics and Electrical Engineering
National Engineering Laboratory
National Institute of Standards and Technology
Boulder, Colorado 80303-3328

August 1989

U.S. DEPARTMENT OF COMMERCE, Robert A. Mosbacher, Secretary
NATIONAL INSTITUTE OF STANDARDS AND TECHNOLOGY, Raymond G. Kammer, Acting Director

CONTENTS

		Page
ABSTRACT		1
INTRODUCTION		1
1.	APD TS System Description	5
2.	Warning When Using the APD TS System	7
3.	APD TS System Parts	7
4.	Power Supplies	8
5.	Setup	8
6.	Operation	9
7.	Making APD TS Measurements	10
8.	Shut-Down	10
9.	APD TS Equipment	10
10.	Calibration Procedures	11
11.	Acknowledgments	14
12.	References	14

Improved Low-Level Silicon-Avalanche-Photodiode Transfer Standards at 1.064 Micrometers.

A.L. Rasmussen, P.A. Simpson, and A.A. Sanders

Electromagnetic Technology Division
National Institute of Standards and Technology
Boulder, Colorado 80303

Three silicon-avalanche-photodiode (APD) transfer standards were calibrated from $\sim 10^{-8}$ to $\sim 10^{-5}$ W/cm^2 peak power density at approximately 10% uncertainty. These calibrations are for 1.064 μm wavelength pulses of 10 to 100 ns duration. For this calibration, an acousto-optically modulated laser beam generated alternately equal levels of pulsed power and cw power into a low-level beam splitter. The cw power measured by a transfer standard in the transmitted beam of the splitter was used to determine the pulsed power into the APD transfer standard in one of the low-level reflected beams of the splitter. The APD detector had about a 1 cm^2 aperture and a 3.8 cm focal length lens in front of it. Lens, window, and detector surfaces had narrow-band antireflection coatings. The commercial detector package is a temperature compensated, infrared-enhanced APD preamplifier module. To increase the sensitivity, one or two 20 dB, 500 MHz bandwidth amplifiers followed the preamplifier. With very low pulsed power, a 30 MHz low-pass filter with Gaussian roll-off was attached to the amplifier output to reduce the noise. A transient digitizer recorded the impulse responses of the APD detectors at 1.064 μm. These data were read into computer programs that convolved the unit-area impulse response with unit-height Gaussian pulses. From these data, correction factors of the pulse peak for observed pulse durations from 10 to 100 ns were determined. Instructions, calibrations, error budgets, and system descriptions are included.

Key words: detector impulse response; laser pulse detectors; laser pulse standards; low-level pulse detectors; pulse power measurements; YAG laser pulse calibrations

INTRODUCTION

Laser designator and range-finder applications have prompted the development of low-level transfer standards at the National Institute of Standards and Technology. The three silicon-avalanche-photodiode transfer standards (APD TS) described in this report have improved sensitivity, stability and accuracy over previous APD transfer standards [1],[2],[3]. Table A, Characteristics of Silicon-Avalanche-Photodiode Transfer Standards (APD TS), and the section that follows give details about these detectors.

DISCLAIMER

Certain commercial equipment, instruments, and materials are identified in this publication in order to explain the experimental procedure adequately. Such identification in no way implies approval, recommendation, or endorsement by the National Institute of Standards and Technology, nor does it imply that the equipment, instruments, or materials identified are necessarily the best available for the purpose.

TABLE A. Characteristics of Silicon-Avalanche-Photodiode Transfer Standards (APD TS)

Parameter	Characteristics
Noise	~4 x 10^{-9} W/cm^2
Range	~10^{-8} to ~10^{-5} W/cm^2
Responsivity	1. Manufacturer's temperature coefficient of responsivity ~0.1% /°C using temperature compensation circuit. 2. Temperature controller 35°C ± ~0.25°C used when environment is severe.
Collector lens	1. Narrow-band 1.064 μm antireflection coating on surfaces. 2. Planoconvex lens with FL 3.8 cm and OD 2.5 cm. 3. Aperture in front of lens approximately 1 cm^2. 4. Lens and detector separated so that collimated beam is a little defocused at the detector. Lens position is read on the scale adjacent to the lens holder, and it is held with a locking nut.
Detector	1. Narrow-band 1.064 μm antireflection coated window and detector. 2. APD-preamplifier module. 3. Dimples in surface of detector to increase internal reflection of beam. 4. Detector uniformity eliminates need for diffuser. 5. Diameter of detector 0.3 cm.
20 dB and 40 dB (two 20 dB units) amplifiers (follow preamplifier)	1. -3 dB BW 500 MHz 2. 20 dB gain (noninverting) DC to 300 MHz 3. Input and output impedance 50 4. Dynamic range 72 dB. 5. Rise and fall times 0.6 to 0.75 ns. 6. Equivalent input noise, 10 Hz to 500 MHz BW, 20 μV. 7. Second and third harmonic distortion -60 dBc (max -50 dBc)
30 MHz filter (follows amplifiers when used)	1. Gaussian roll-off 2. Lowpass 3. 3 dB cut-off frequency, 30 MHz.

1. APD TS System Description.

These transfer standards will measure ~10^{-8} to 10^{-5} W/cm^2 peak power density of ~10 to 100 ns duration pulses at 1.064 μm wavelength. See figure 1.

The detector package is a specially ordered commercial unit. An antireflection coated lens and fixed aperture are mounted in front of the 3 mm diameter detector, which has an antireflection coated window. The complete unit is housed in a black box with attached legs and platform.

Power supplies are provided for the detector, preamplifier, amplifiers, and temperature controller. Temperature compensation in the detector package maintains the responsivity with negligible change over a broad temperature range. The temperature controller was designed to maintain the detector at a given temperature when needed.

The detector unit is a temperature compensated silicon-avalanche-photodiode preamplifier module. The detector is IR-enhanced and has an array of dimples on its surface. These dimples and an antireflection coating on the detector surface increase the signal absorption and responsivity. Because of the dimples the responsivity will show nonuniformity when the surface is scanned with a very small beam. Using a 0.3-0.4 cm diameter beam that was focused to a small spot, we calibrated the detector at the center of the surface. It

was also calibrated at seven mathematically selected locations[1] on the surface to determine the uniformity of the responsivity with the given beam. APD 721 and APD 723 were rotated 45° and calibrated at seven locations again.

From these data the center calibration was given a correction factor and uncertainty for the uniformity.

When a ~10 cm diameter, stable, uniform, collimated LED beam was directed into the detector with 0.5 cm^2 and 1 cm^2 apertures, the detector output was proportional to the area of these apertures. The responsivity of the detector was uniform to these larger beams.

To increase the sensitivity of detection, one or two amplifiers are attached to the preamplifier output. These may be followed by a 30 MHz low-pass filter with Gaussian roll-off to reduce noise and to measure ~10^{-8} w/cm^2 peak power density of ~20 ns duration pulses. Since the filter lengthens the impulse response time of the system, the correction factor for the peak voltage changes accordingly.

At 1.064 μm correction factors for peak voltage at the observed pulse duration are given for 0 dB, 20 dB (with and without the 30 MHz low-pass filter), and 40 dB (with the 30 MHz low-pass filter).

---

[1] Handbook of Mathematical Functions, U.S. Department of Commerce, National Bureau of Standards, AMS 55. Edited by M. Abramowitz and Irene A. Stegun, June 1964, p 892. Weighted average of seven points in circular area with h = 0.4 cm was the same as the average of the seven values. Rotating the detectors 45° and taking seven more points yielded similar averages.

2. Warning When Using the APD TS System

a. Stay within the power and voltage ranges in the table of the APD TS system.

b. Do not exceed these limits for you can burn out components in the APD TS system and cost considerable expense and time to repair, replace, and recalibrate.

c. Do not disassemble the APD TS for you can ruin its calibration.

d. Operate the APD TS in a darkened room to prevent instrument damage and erroneous measurements.

e. Observe input/output connections of amplifier(s) and the 30 MHz low-pass filter.

f. Stay within the ranges given for the amplifiers. You can damage them if you exceed these limits. Also, just slightly exceeding these limits can introduce subtle errors.

3. APD TS System Parts.

a. APD TS with built in lens and aperture.
b. Alignment mirror and iris.
c. Two lens mount sleeves.
d. Detector bias power supply.
e. Preamplifier bias power supply.
f. Temperature controller power supply.
g. Temperature measuring equipment (digital voltmeter provided by user).
h. Ungrounded precision voltmeter (provided by user).
i. Two 20 dB amplifiers with power supply attached.
j. 30 MHz filter.
k. Cables.

4. Power Supplies

a. Preamplifier bias power supply, ± 9.0 V.

b. Detector bias power supply, + 550.0 V. Turn on or off by gradually increasing or decreasing voltage.

c. Temperature controller power supply, + 15 V (not generally used because temperature compensator circuit of the detector maintains a calibration that changes negligibly over a broad temperature range).

5. Setup

a. Do not connect the temperature controller power supply and temperature meter to the detector unless temperature control is needed.

b. If you need temperature control, connect the temperature controller to the detector, and a digital ohmmeter (operating temperature reading about 3.5 kΩ) to the temperature meter terminal of the detector.

c. Attach detector bias power supply to the detector + 550.0 V terminal and to an ungrounded precision voltmeter (furnished by user).

d. Attach preamplifier power supply to the appropriate terminal of the detector using the flexible grey cable.

e. Attach output terminal of the detector to a 7A24 oscilloscope plug-in of a 7904 oscilloscope or equivalent for 0 dB gain measurements or to the 20 dB amplifier for 20 dB gain or the two 20 dB amplifiers in series for 40 dB gain. Attach amplifiers in order of serial numbers given in calibration tables 1-3, see footnote †.

f. For lower noise attach the 30 MHz low-pass filter to the output of the amplifier(s).

g. For wider bandwidth attach the 20 dB amplifier with serial number given in the calibration tables 1-3, see footnote †, without the 30 MHz low-pass filter.

h. Attach the amplifier or 30 MHz low-pass filter output to the oscilloscope plug-in.

i. Observe input/output connections of amplifier(s) and the 30 MHz low-pass filter.

6. Operation

a. Turn on preamplifier power supply.

b. Turn on detector bias power supply, gradually increasing voltage until it reads exactly the operating voltage. Return the voltage to zero in a like manner when shutting off equipment.

c. Turn on amplifiers being used, and disconnect and turn them off when changing or shutting off equipment.

d. Remove the alignment mirror from the detector.

e. Blow dust off the APD collector with a squeeze-type air blower ONLY (other types such as those in spray cans may spray liquid and damage the surface).

f. Reattach the alignment mirror and attach the iris.

g. Align the APD TS in a visible or 1.064 μm beam with the beam returning on itself, or

h. Using a collimated beam, align the APD TS without the alignment mirror and iris by positioning it for maximum pulse height at a gain and range given in the calibration table.

7. Making APD TS Measurements

a. Set a baseline of two divisions and a pulse height of three to five divisions.

b. Refer to tables 1, 2, 3, and 4 for gain, calibration, range, and uncertainty.

c. Read the peak voltage and the observed pulse duration (FDHM).

d. Find the corrected peak voltage by multiplying the observed value by the correction factor in figures 2 through 13.

e. Divide the corrected peak voltage by the calibration in column 1 of tables 1, 2, or 3 to get the power density (W/cm^2).

f. Acquire enough data for significant statistical information.

8. Shut-Down

a. Disconnect and turn off the amplifier(s).

b. Gradually decrease the voltage of the detector bias power supply to zero and turn the power supply off.

c. Turn off the preamplifier power supply.

d. Reattach the alignment mirror to the APD TS to protect the collector of the detector.

9. APD TS Equipment

a. APD detector bias power supply, Bertan Assoc. Inc., Model 602B-15P.

b. Precision digital voltmeter for detector bias voltage measurement.

c. CLC100 linear amplifiers, Comlinear Corporation.

d. Oscilloscope readout, Tektronix 7904, NIST 145935 (used at NIST).
   1. APD readout, dual trace amplifier, 7A24, 50Ω.
   2. Dual time base, 7B92A.

e. Preamplifier bias power supply (NIST made).

f. Temperature controller power supply (NIST made).

g. Low-pass filter, 3 dB cutoff frequency 30 MHz, Gaussian roll-off; Reactel, Inc., Model 7LX4-30-B21.

10. Calibration Procedures

a. Responsivity.

Procedures for calibrating responsivity have been described in several publications [1-4], and are briefly reviewed here. An acousto-optically modulated cw 1.064 μm laser beam in the TEM_{00} mode generates alternately equal levels of pulsed power and cw power into a low-level beam splitter. The cw power measured by a transfer standard in the transmitted beam of the splitter is used to determine the pulsed power into the APD transfer standard in one of the reflected beams of the splitter. The calibration factor is found by dividing the peak output voltage by the pulsed power per aperture area of the APD collector.

b. Impulse response related corrections of the peak voltage of the APD transfer standards.

A transient digitizer recorded the impulse responses of the APD transfer standards. These data were read into computer programs that convolved the unit-area impulse response with unit-height Gaussian pulses of various selected durations. From these data, correction factors of the pulse peak for observed pulse durations from 10 to 100 ns were determined.

Inserting a 30 MHz filter in the detector system reduces noise and increases sensitivity. However, the correction factor for the peak voltage and its uncertainty also increase, especially for the shorter pulses. See correction factor curves, figures 2 through 13.

Use the following measurements and equations to calibrate directly the correction factor for the peak voltage with the 40 dB amplifier and 30MHz filter: (1) Measure peak power near the bottom of the range with the 20 dB amplifier and no filter and (2) Determine the correction factor for the peak voltage with the peak power unchanged and near the top of the range with the 40 dB amplifier and the 30 MHz filter.

Apply the following equations:

$$W_p = \frac{CF_{20} \quad V_{p20}}{K_{20}}$$

near the bottom of the range with the 20 dB amplifier and <u>no</u> filter

where

W_p = peak power in watts

CF_{20} = correction factor of peak voltage with 20 dB amplifier (see figs. 2-13)

V_{p20} = peak voltage reading with 20 dB amplifier

K_{20} = calibration factor with 20 dB amplifier (see tables 1, 2, or 3, column 1);

and

$$W_p = \frac{CF_{40F} \quad V_{p40F}}{K_{40F}}$$

near the top of the range with the 40 dB amplifier and the filter where

W_p = peak power, as before

CF_{40F} = correction factor of peak voltage with 40 dB amplifier and 30 MHz filter (to be calculated)

K_{40F} = calibration factor with 40 dB amplifier and 30 MHz filter (see tables 1, 2, or 3, column 1)

V_{p40F} = peak voltage with 40 dB amplifier and 30 MHz filter corresponding to an observed pulse duration.

From these equations we get the correction factor

$$CF_{40F} = \frac{W_p \; K_{40F}}{V_{p40F}}$$

If the laser pulse maintains its shape, then CF_{40F} is constant over the range of the detector with 40 dB amplifier and 30 MHz filter.

Curves of correction factor of peak voltage versus observed pulse duration for identical gain and measurement parameters are very repeatable. However, correction factors at the highest peak power range (0 dB) differ for changes in level of the Gaussian impulse response. These differences diminish rapidly with increased pulse duration. See tables 5, 6, and 7. They are due to load differences when changing gain settings of the transient digitizer during impulse response measurements.

For a given gain and set of measurement parameters of APD 721, the convolution of the impulse response with Gaussian, skewed Gaussian, and cosine-squared input pulses at a given observed pulse duration

yield approximately the same correction factors of the peak voltage. See tables 8 through 11. Convolution with triangular and rectangular (not shown) input pulses yield more scattered correction factors of the peak voltage from the above.

11. Acknowledgments

The authors thank J.J. Skudler for designing and fabricating transfer standard components. They also thank the Aerospace Guidance and Metrology Center, Newark Air Force Station for funding this work.

12. References

[1] Sanders, A. A.; Rasmussen, A. L. A system for measuring energy and peak power of low-level 1.064 μm laser pulses. NBS Tech. Note 1058 (1982).

[2] Rasmussen, A. L.; Sanders, A. A. Transfer standards for energy and peak power of low-level 1.064 micrometer pulses and continuous wave laser power. Optical Engineering 25(2), 277-285; 1986 February.

[3] Rasmussen, A. L.; Sanders, A. A. Documentation of the NBS APD and PIN calibration systems for measuring peak power and energy of low-level 1.064 μm laser pulses. NBSIR 85-3032, 1985 December.

[4] Rasmussen, A. L.; Franzen, D. L. Low-level germanium detector transfer standard at 1.064 μm. NBSIR 85-3041, 1986 January.

TABLE 1. APD 721 SYSTEM CALIBRATION*

	Calibration $V \cdot cm^2/W$ * ** †	Number of calibrations n	Uncertainty in the average of the measurements $SD/\sqrt{n}$ %	Total estimated uncertainty $3\sqrt{(SD)^2/n + \sum_1^5 S_i{}^2/3}$ %	Power range $\mu W/cm^2$ **	Readout range V
(1)	1.72×10^4	32	0.33	10.9	1.1-26	0.019-0.44
(2)	1.63×10^5	34	0.47	10.9	0.11-5.1	0.018-0.81
(3)	1.55×10^6	29	0.33	10.9	0.024-0.54	0.037-0.85

* Calibrations February and March, 1987.

** Aperture area 1.027 cm^2, lens set 1 mm below R.

† TX 7904 oscilloscope, Ch 2, 7A24 50 Ω plug-in:
(1) 0 dB.
(2) 20 dB, amplifier, SN 22210 with and without 30 MHz filter, SN 87-1. Without filter noise 0.03 $\mu W/cm^2$.
(3) 40 dB, amplifiers, SN 22210 and SN 22209 with 30 MHz filter, SN 87-1. Noise 0.004 $\mu W/cm^2$.

Correction factors were applied to calibration averages:

Uniformity calibration average/
Center of detector calibration average,
for APD 721, APD 723, and APD 725 =

1.002, 0.992, 1.014 resp.

TABLE 2. APD 723 SYSTEM CALIBRATION*

	Calibration $V \cdot cm^2/W$ * ** †	Number of calibrations n	Uncertainty in the average of the measurements $SD/\sqrt{n}$ %	Total estimated uncertainty $3\sqrt{(SD)^2/n + \sum_1^5 S_i^2/3}$ %	Power range $\mu W/cm^2$ **	Readout range V
(1)	1.59×10^4	52	0.30	10.5	1.2-29	0.020-0.45
(2)	1.50×10^5	40	0.26	10.5	0.12-5.3	0.018-0.82
(3)	1.45×10^6	26	0.23	10.5	0.027-0.55	0.040-0.80

* Calibrations February and March, 1987.

** Aperture area 1.028 cm^2, lens set 2 mm below R.

† TX 7904 oscilloscope, Ch 2, 7A24 50 Ω plug-in:
(1) 0 dB.
(2) 20 dB, amplifier, SN 22015 with and without 30 MHz filter, SN 87-2. Without filter noise 0.03 $\mu W/cm^2$.
(3) 40 dB, amplifiers, SN 22015 and SN 22014 with 30 MHz filter, SN 87-2. Noise 0.004 $\mu W/cm^2$.

Correction factors were applied to calibration averages:

Uniformity calibration average/
Center of detector calibration average,
for APD 721, APD 723, and APD 725 =

1.002, 0.992, 1.014 resp.

TABLE 3. APD 725 SYSTEM CALIBRATION*

	Calibration $V \cdot cm^2/W$ * ** †	Number of calibrations n	Uncertainty in the average of the measurements $SD/\sqrt{n}$ %	Total estimated uncertainty $3\sqrt{(SD)^2/n + \sum_1^5 S_i^2/3}$ %	Power range $\mu W/cm^2$ **	Readout range V
(1)	1.55×10^4	30	0.18	10.2	1.2-28	0.019-0.43
(2)	1.43×10^5	18	0.27	10.2	0.14-5.6	0.019-0.78
(3)	1.40×10^6	27	0.25	10.2	0.029-0.56	0.040-0.77

* Calibrations February and March, 1987.

** Aperture area 1.025 cm^2, lens set 1½ mm below R.

† TX 7904 oscilloscope, Ch 2, 7A24 50 Ω plug-in:
(1) 0 dB.
(2) 20 dB, amplifier, SN 22220 with and without 30 MHz filter, SN 87-3. Without filter noise 0.03 $\mu W/cm^2$.
(3) 40 dB, amplifiers, SN 22220 and SN 22016 with 30 MHz filter, SN 87-3. Noise 0.004 $\mu W/cm^2$.

Correction factors were applied to calibration averages:

Uniformity calibration average/
Center of detector calibration average,
for APD 721, APD 723, and APD 725 =

1.002, 0.992, 1.014 resp.

TABLE 4. Error budget APD 721, APD 723, and APD 725 system.

Source of error	Uncertainty %
Redw 3 transfer standard(identifying designation to commercial instrument), S_1	1.9
Beamsplitter attenuator, S_2	2.5
Equivalence of pulsed and cw power, S_3	2.5
Oscilloscope readout, S_4	3.0
Correction factor of peak voltage for OBS Δt (observed pulse duration) ≥ 15 ns, S_5	3.0
$\sqrt{\sum_1^5 S_i^2/3}$	3.37

Precision and uniformity, $(SD)/\sqrt{n}$:

$(SD)_1/\sqrt{n_1}$ (APD 721), $(SD)_2/\sqrt{n_2}$ (APD 723), and $(SD)_3/\sqrt{n_3}$ (APD 725) =

1.38, 0.88, 0.37 resp.

Total uncertainty for APD 721, APD 723, and APD 725:

$$3\sqrt{(SD)^2/n+\sum_1^5 S_i^2/3} = \quad 10.9, \quad 10.5, \quad 10.2 \text{ resp.}$$

TABLE 5. Percent deviation of average CF V_p* from CF V_p data of individual runs (see Fig. 2)

APD 721 - 0 dB - No Filter

Input Gaussian pulse duration ns	Average CF V_p*† of runs 9 & 10	Average OBS Δt**† of runs 9 & 10	Percent deviation of average CF V_p* from CF V_p of runs 9 & 10	Impulse response peak voltage
10	0.961	9.6	± 1.4	Run 9, 203 mV
15	0.987	14.6	0.8	Run 10, 20.1 mV
20	0.999	19.7	0.4	
25	1.005	24.8	0.2	
30	1.007	29.9	0.1	
35	1.008	35.0	0.1	
40	1.009	40.1	0	
50	1.008	50.3	0	
60	1.007	60.3	0	
70	1.006	70.3	0	
80	1.005	80.3	0	
90	1.004	90.3	0	
100	1.003	100.3	0	

* CF V_p = correction factor peak voltage
** OBS Δt = observed pulse duration
† Correcting the impulse response for transient digitizer calibration yielded identical values of CF V_p and OBS Δt.

TABLE 6. Percent deviation of average CF V_p* from CF V_p data of individual runs (see Fig. 6)

APD 723 - 0 dB - No Filter

Input Gaussian pulse duration ns	Average CF V_p*† of runs 16 & 17	Average OBS Δt**† of runs 16 & 17	Percent deviation of average CF V_p* from CF V_p of runs 16 & 17	Impulse response peak voltage
10	0.964	9.74	± 3.2	Run 16, 20.9 mV
15	0.982	14.6	2.3	Run 17, 206 mV
20	0.994	19.7	1.7	
25	0.999	24.7	1.4	
30	1.002	29.8	1.2	
35	1.004	34.9	1.0	
40	1.005	40.0	0.9	
50	1.005	50.1	0.7	
60	1.004	60.2	0.6	
70	1.004	70.2	0.4	
80	1.003	80.2	0.4	
90	1.002	90.2	0.3	
100	1.002	100.2	0.2	

* CF V_p = correction factor peak voltage

** OBS Δt = observed pulse duration

† Correcting the impulse response for transient digitizer calibration yielded identical values of CF V_p and OBS Δt.

TABLE 7. Percent deviation of average CF V_p* from CF V_p data of individual runs (see Fig. 10)

APD 725 - 0 dB - No Filter

Input Gaussian pulse duration ns	Average CF V_p*† of runs 1 & 4	Average OBS Δt**† of runs 1 & 4	Percent deviation of average CF V_p* from CF V_p of runs 1 & 4	Impulse response peak voltage
10	0.962	9.72	± 2.2	Run 1, 204 mV
15	0.980	14.7	1.5	Run 4, 19.7 mV
20	0.990	19.7	1.2	
25	0.995	24.8	0.9	
30	0.998	29.8	0.8	
35	0.999	34.9	0.7	
40	1.000	39.9	0.7	
50	1.001	50.0	0.5	
60	1.001	60.0	0.4	
70	1.001	70.0	0.3	
80	1.001	80.1	0.3	
90	1.001	90.1	0.2	
100	1.001	100.1	0.2	

* CF V_p = correction factor peak voltage

** OBS Δt = observed pulse duration

† Correcting the impulse response for transient digitizer calibration yielded identical values of CF V_p and OBS Δt.

TABLE 8. CF V_p* as a function of observed pulse duration (OBS Δt) and input pulse shape (Table derived from interpolation of graphed data)

APD 721 - 0 dB - No Filter - Run 10

Observed pulse duration (OBS Δt)	CF V_p* Gaussian input pulse	CF V_p* Skewed** Gaussian input pulse	CF V_p* Cosine-squared input pulse	CF V_p* Triangular input pulse
10	0.949	0.932	0.948	1.042
15	0.981	0.963	0.980	1.032
20	0.996	0.985	0.997	1.028
25	1.004	0.997	1.004	1.027
30	1.006	1.003	1.007	1.024
35	1.008	1.006	1.01	1.023
40	1.01	1.008	1.012	1.02
50	1.01	1.01	1.01	1.017

TABLE 9. CF V_p* as a function of observed pulse duration (OBS Δt) and input pulse shape (Table derived from interpolation of graphed data)

APD 721 - 20 dB - No Filter - Run 11

Observed pulse duration (OBS Δt)	CF V_p* Gaussian input pulse	CF V_p* Skewed** Gaussian input pulse	CF V_p* Cosine-squared input pulse	CF V_p* Triangular input pulse
10	0.921	0.914	0.921	1.022
15	0.958	0.943	0.962	1.006
20	0.973	0.963	0.972	1.010
25	0.982	0.975	0.986	1.007
30	0.988	0.982	0.989	1.006
35	0.992	0.987	0.994	1.006
40	0.994	0.990	0.994	1.005
50	0.996	0.994	0.997	1.004

* CF V_p = correction factor peak voltage

** Skewed Gaussian pulses had a Gaussian right side with a FWHM 40% longer than a Gaussian left side.

TABLE 10. CF V_p* as a function of observed pulse duration (OBS Δt) and input pulse shape (Table derived from interpolation of graphed data)

APD 721 - 20 dB - Filter - Run 12

Observed pulse duration (OBS Δt)	CF V_p* Gaussian input pulse	CF V_p* Skewed** Gaussian input pulse	CF V_p* Cosine-squared input pulse	CF V_p* Triangular input pulse
16	1.418	1.427	1.373	1.524
20	1.178	1.193	1.147	1.279
25	1.091	1.090	1.067	1.182
30	1.055	1.051	1.039	1.143
35	1.033	1.033	1.029	1.122
40	1.022	1.023	1.022	1.103
50	1.008	1.010	1.008	1.070

TABLE 11. CF V_p* as a function of observed pulse duration (OBS Δt) and input pulse shape (Table derived from interpolation of graphed data)

APD 721 - 40 dB - Filter - Run 13

Observed pulse duration (OBS Δt)	CF V_p* Gaussian input pulse	CF V_p* Skewed** Gaussian input pulse	CF V_p* Cosine-squared input pulse	CF V_p* Triangular input pulse
16	1.462	-	1.428	1.550
20	1.153	1.170	1.121	1.248
25	1.050	1.050	1.032	1.149
30	1.019	1.014	1.004	1.108
35	1.003	0.998	0.994	1.087
40	0.995	0.992	0.992	1.073
50	0.987	0.985	0.986	1.052

* CF V_p = correction factor peak voltage

** Skewed Gaussian pulses had a Gaussian right side with a FWHM 40% longer than a Gaussian left side.

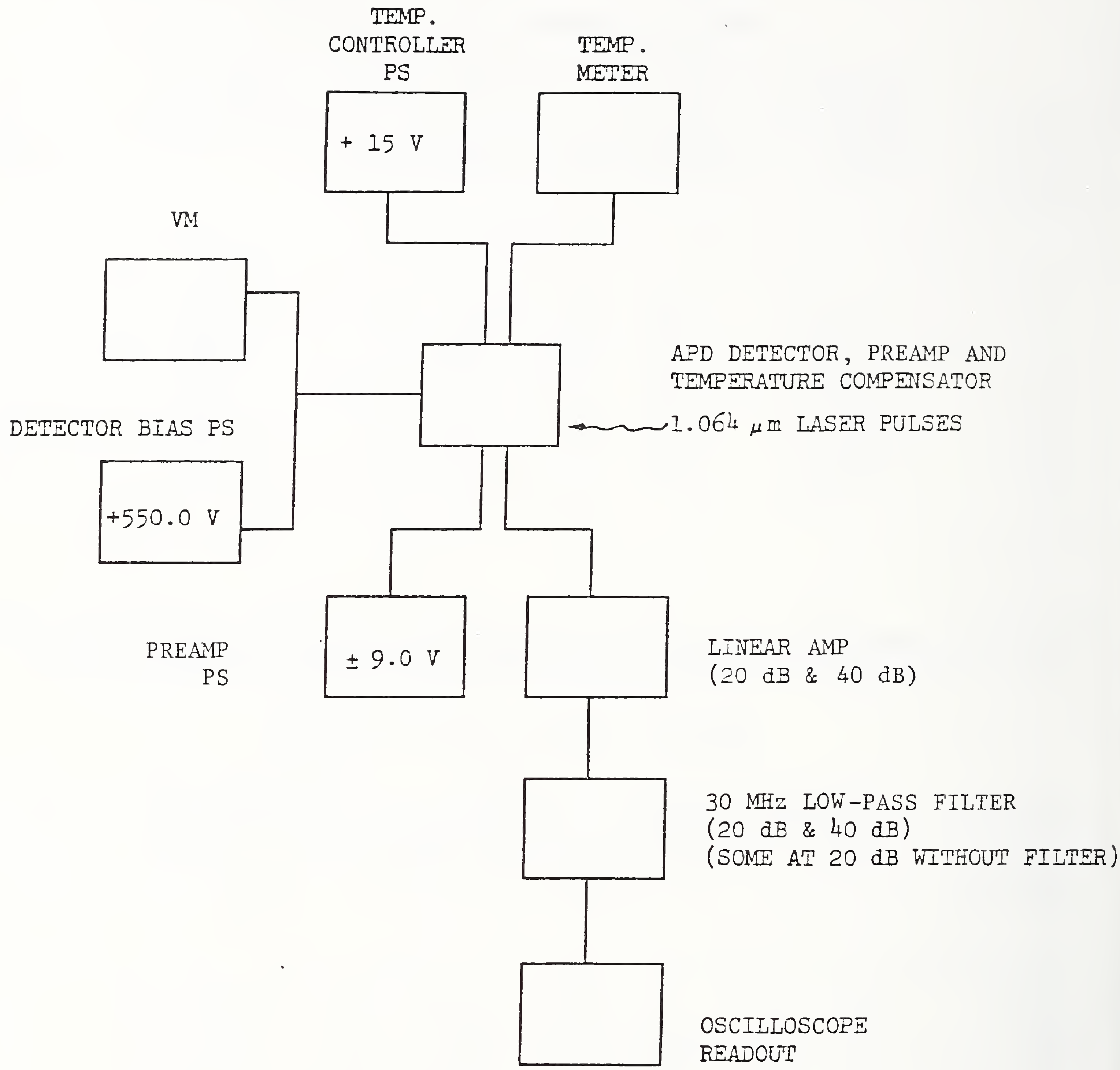

Figure 1. APD Transfer Standard System

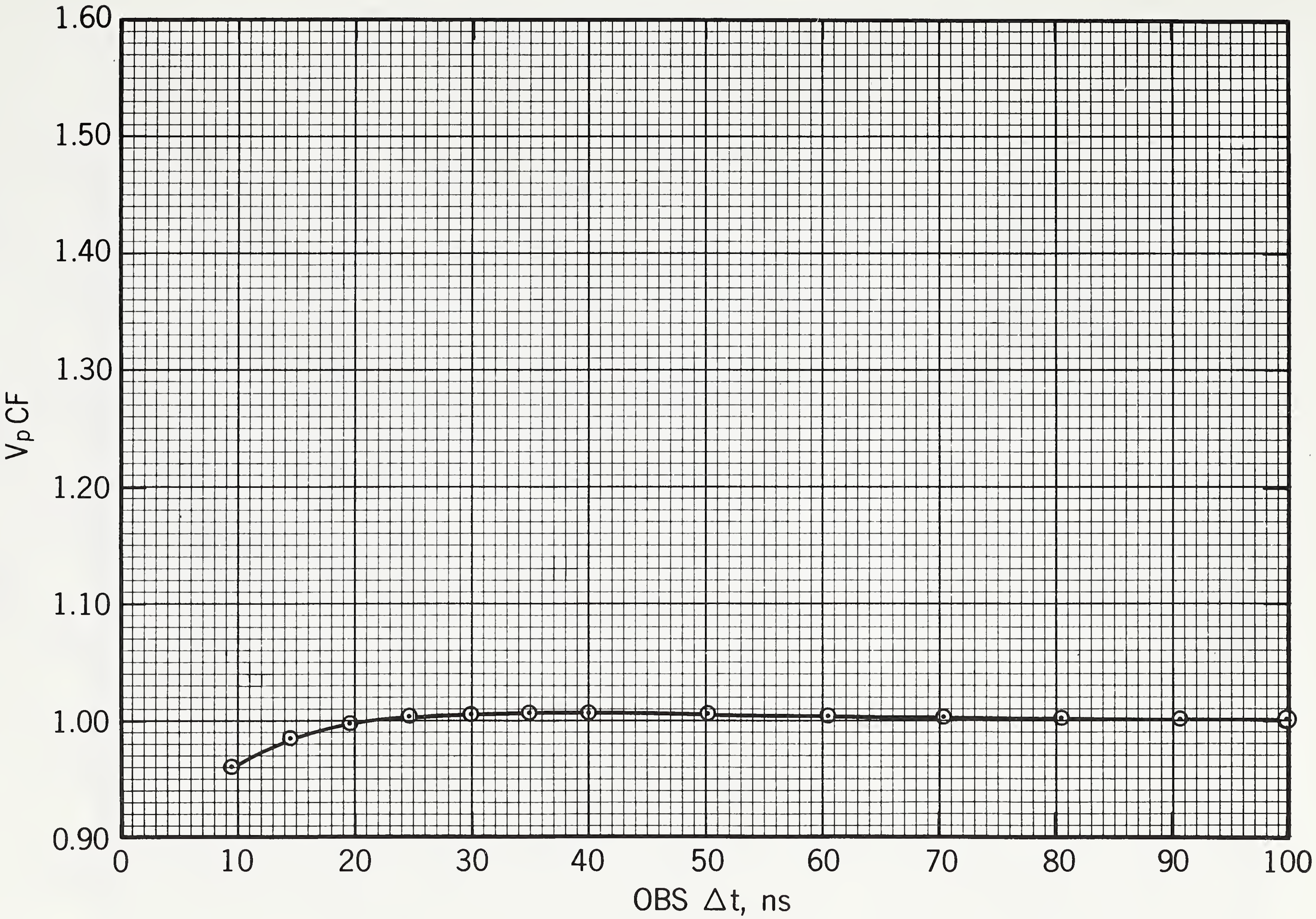

Figure 2. APD 721 - 0 dB - No Filter. (Average of runs 9 and 10). Average values of peak voltage correction factor (V_p CF) versus observed pulse duration (OBS Δt) in ns for impulse response maximum of 203 mV and 20.1 mV.

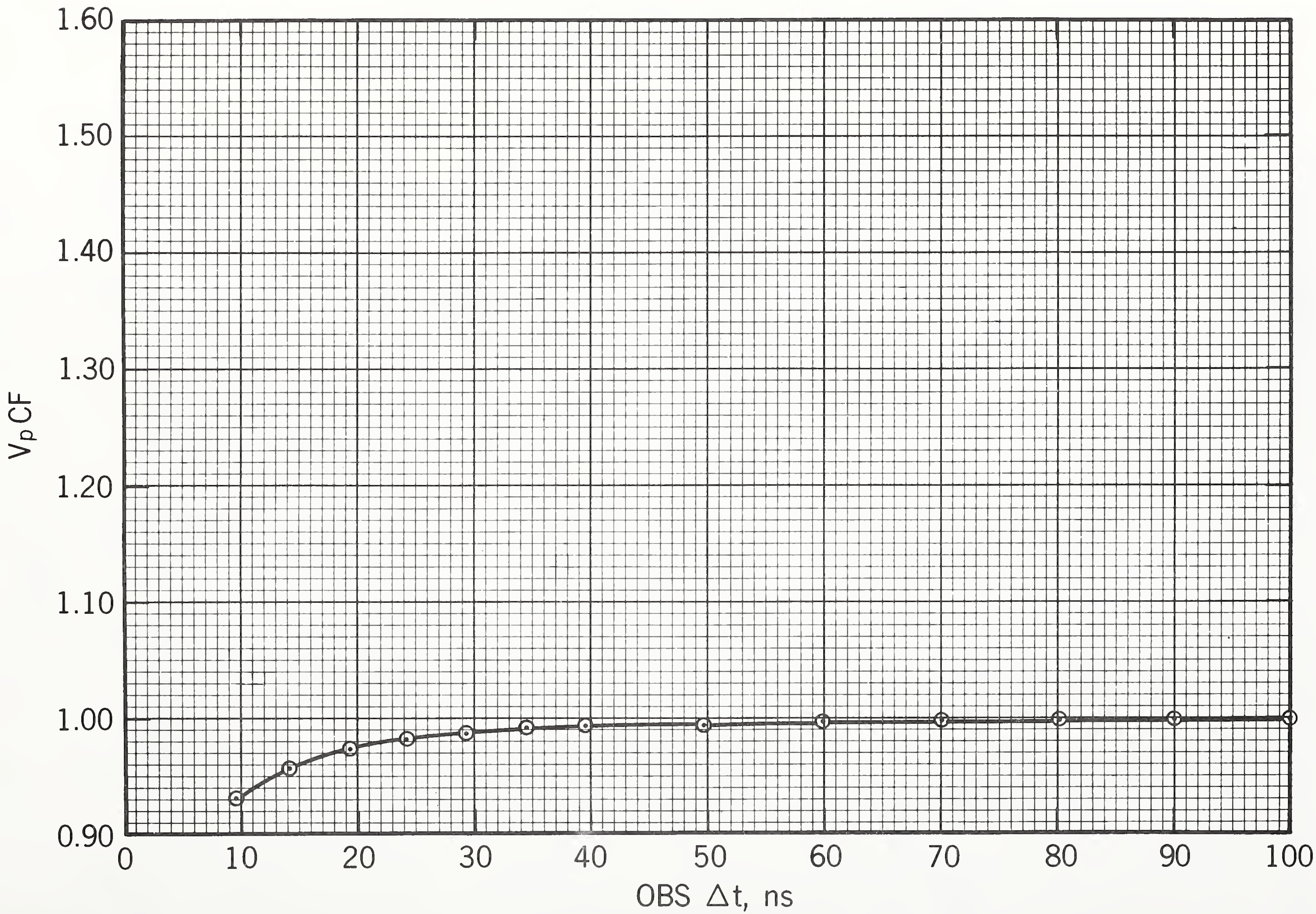

Figure 3. APD 721 - 20 dB - No Filter - Run 11
Peak voltage correction factor (V_p CF) versus observed pulse duration (OBS Δt) for impulse response maximum of 195 mV.

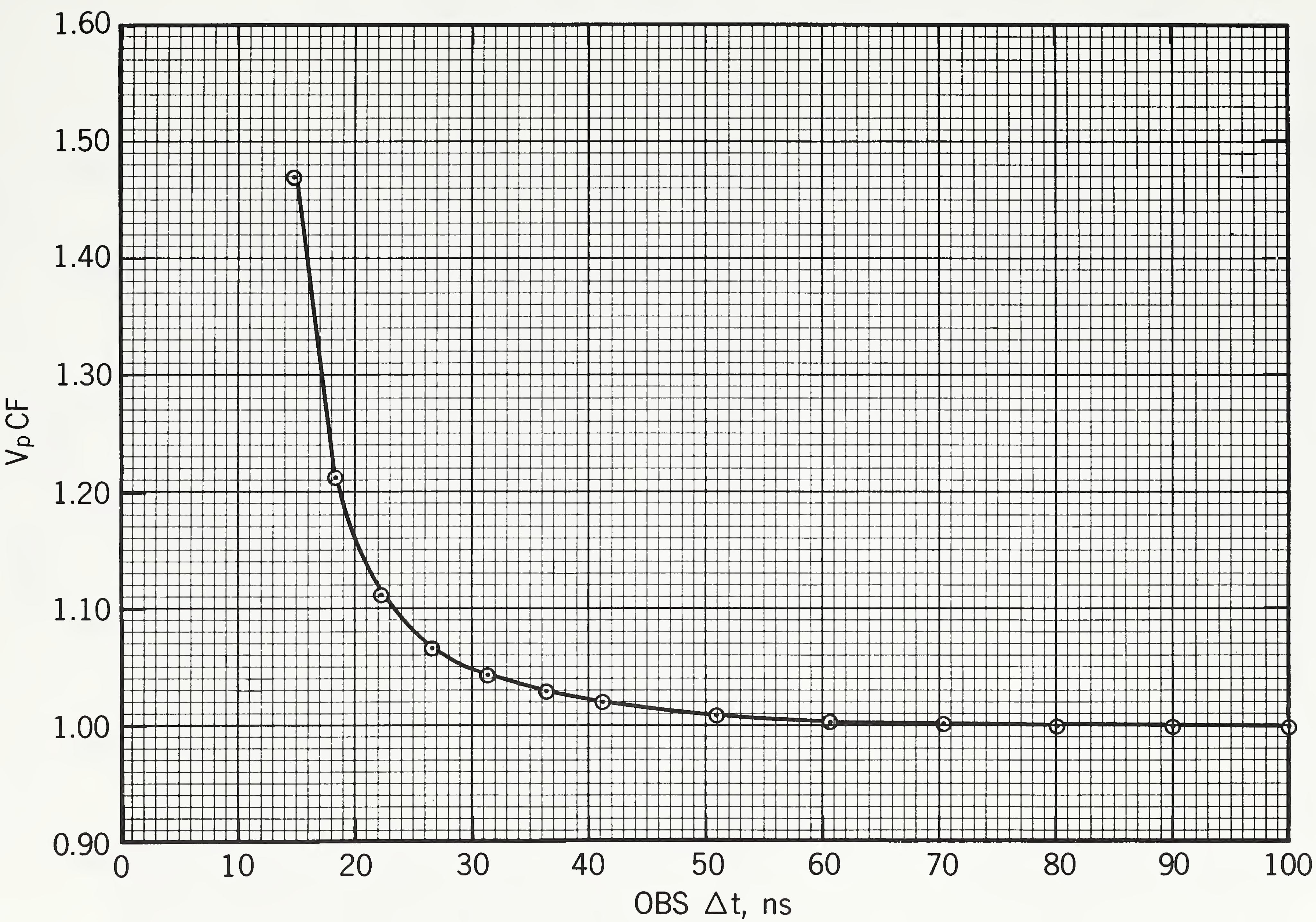

Figure 4. APD 721 - 20 dB - Filter - Run 12
Peak voltage correction factor (V_p CF) versus observed pulse duration (OBS Δt) for impulse response maximum of 52.7 mV.

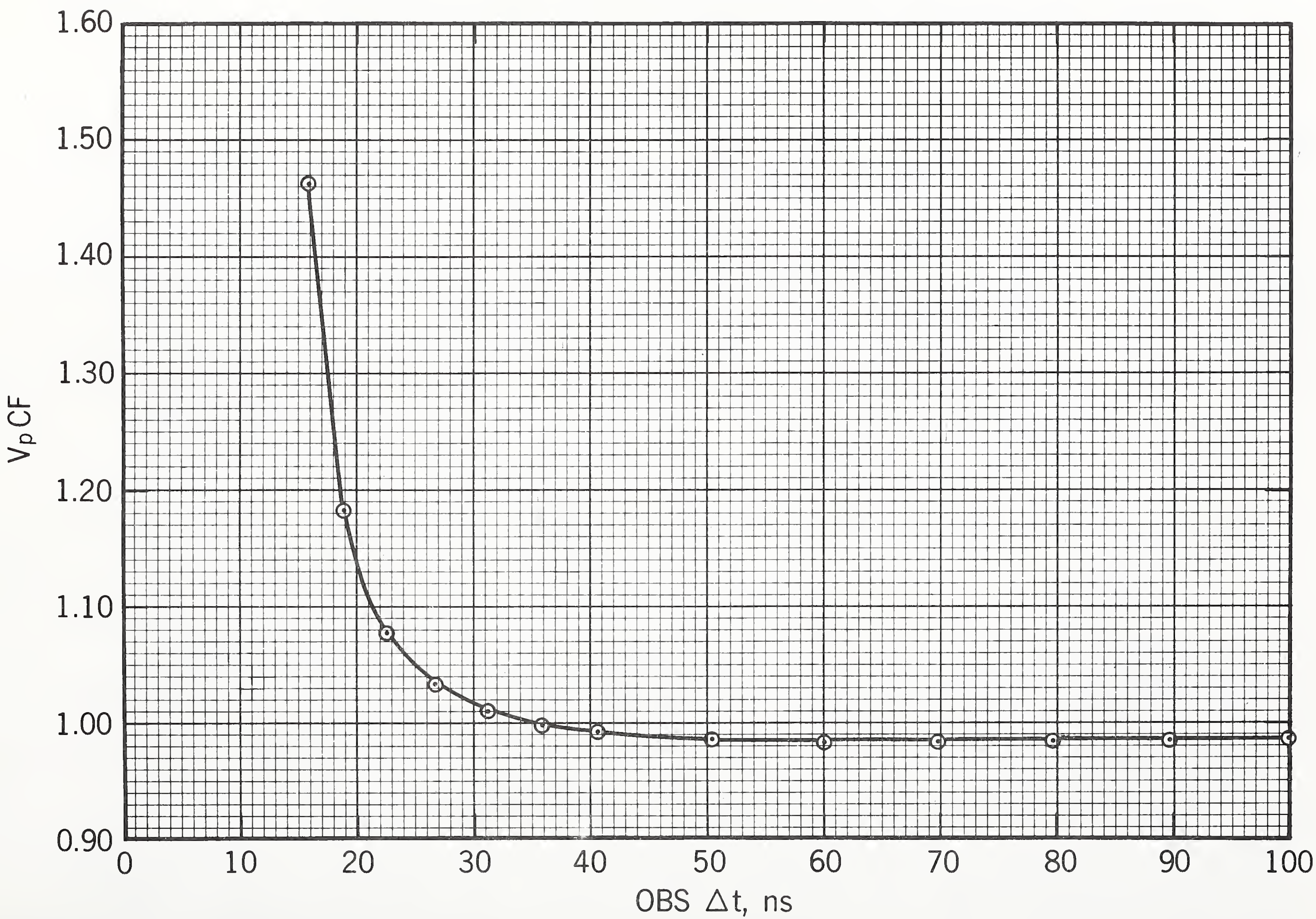

Figure 5. APD 721 - 40 dB - Filter - Run 13
Peak volatage correction factor (V_p CF) versus observed pulse duration (OBS Δt) for impulse response maximum of 147 mV.

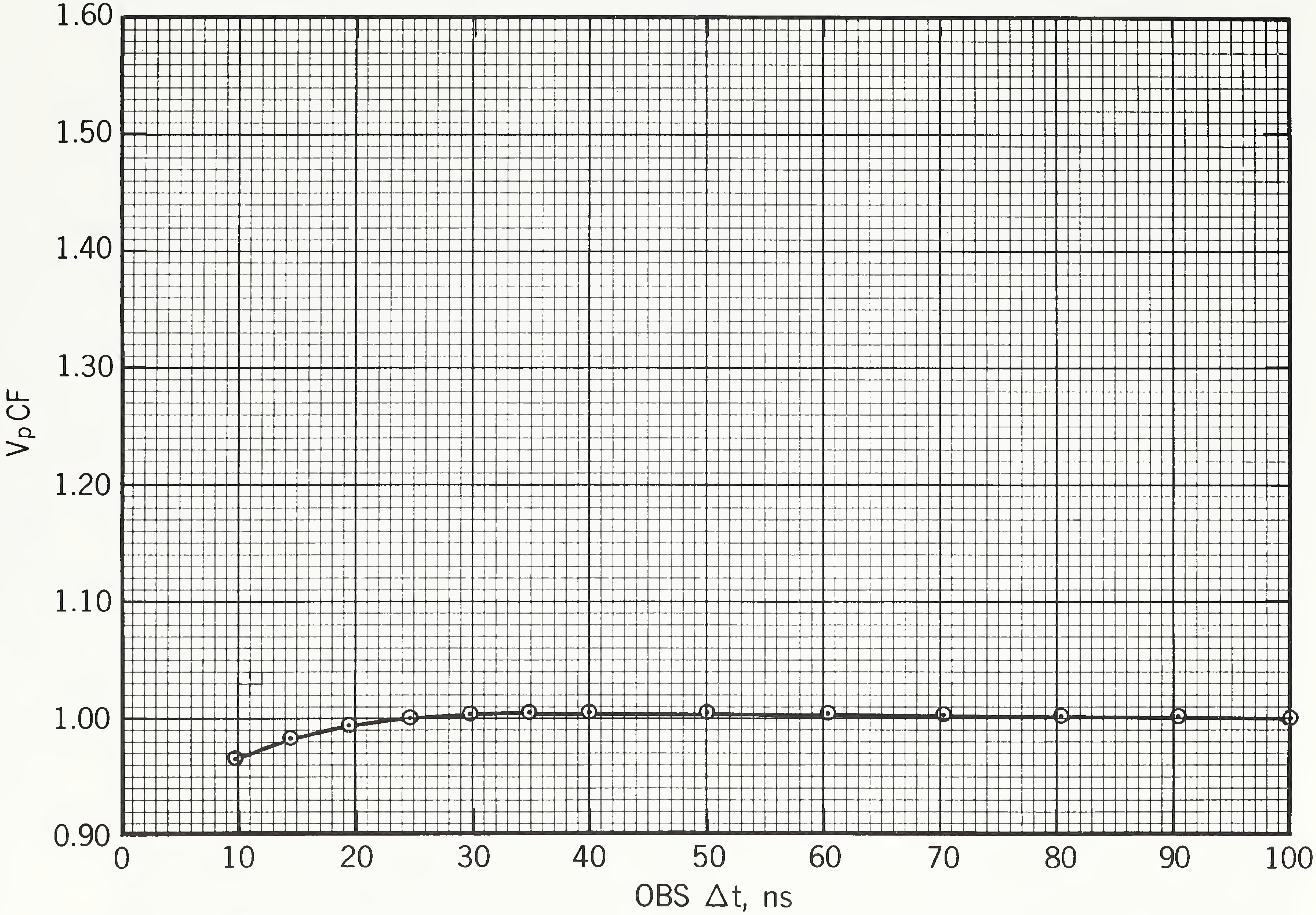

Figure 6. APD 723 - 0 dB - No Filter. (Average of runs 16 and 17). Average values of peak voltage correction factor (V_p CF) versus observed pulse duration (OBS Δt) in ns for impulse response maximum of 209 mV and 20.6 mV.

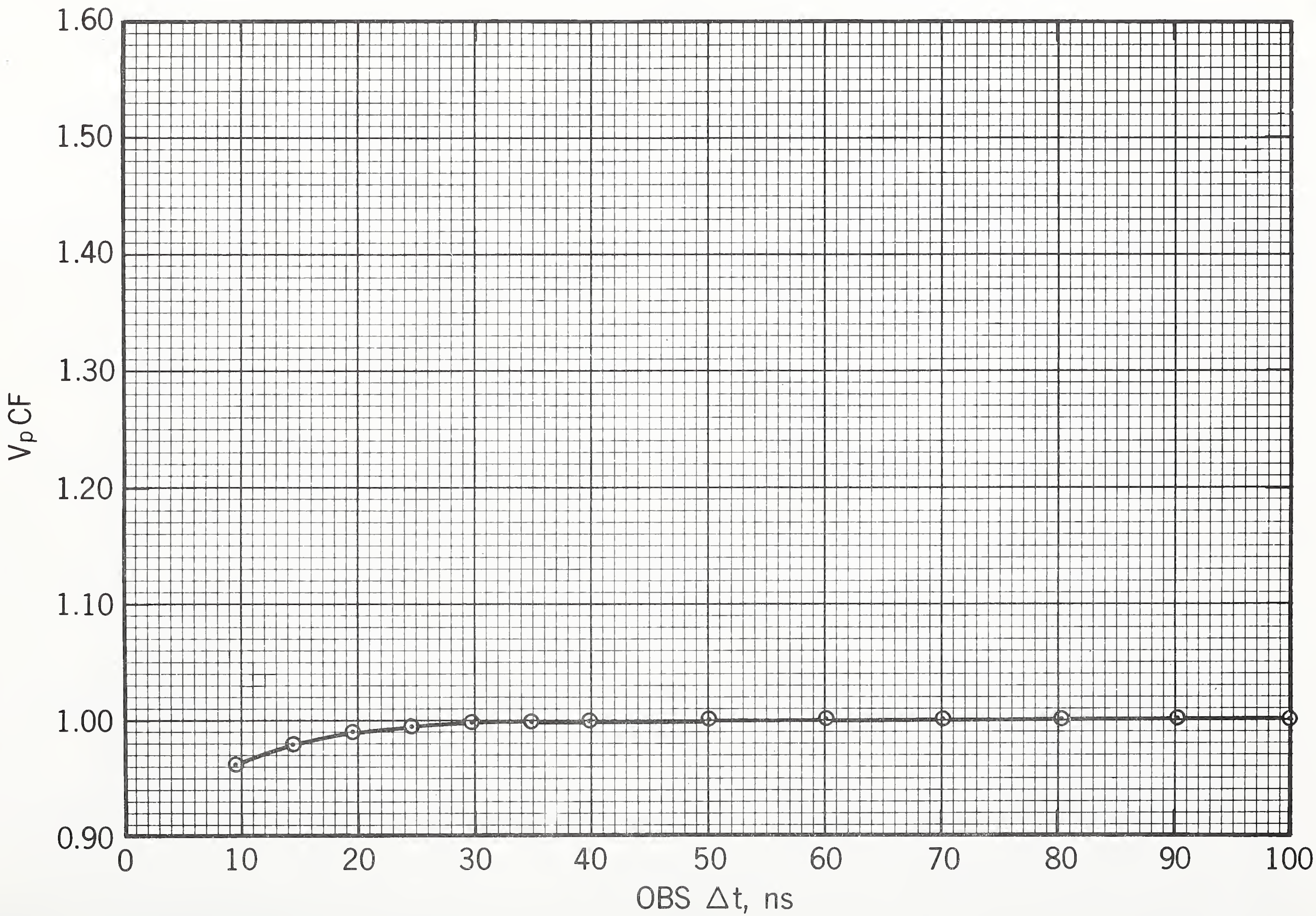

Figure 7. APD 723 - 20 dB - No Filter - Run 19
Peak voltage correction factor (V_p CF) versus observed pulse duration (OBS Δt) for impulse response maximum of 199 mV.

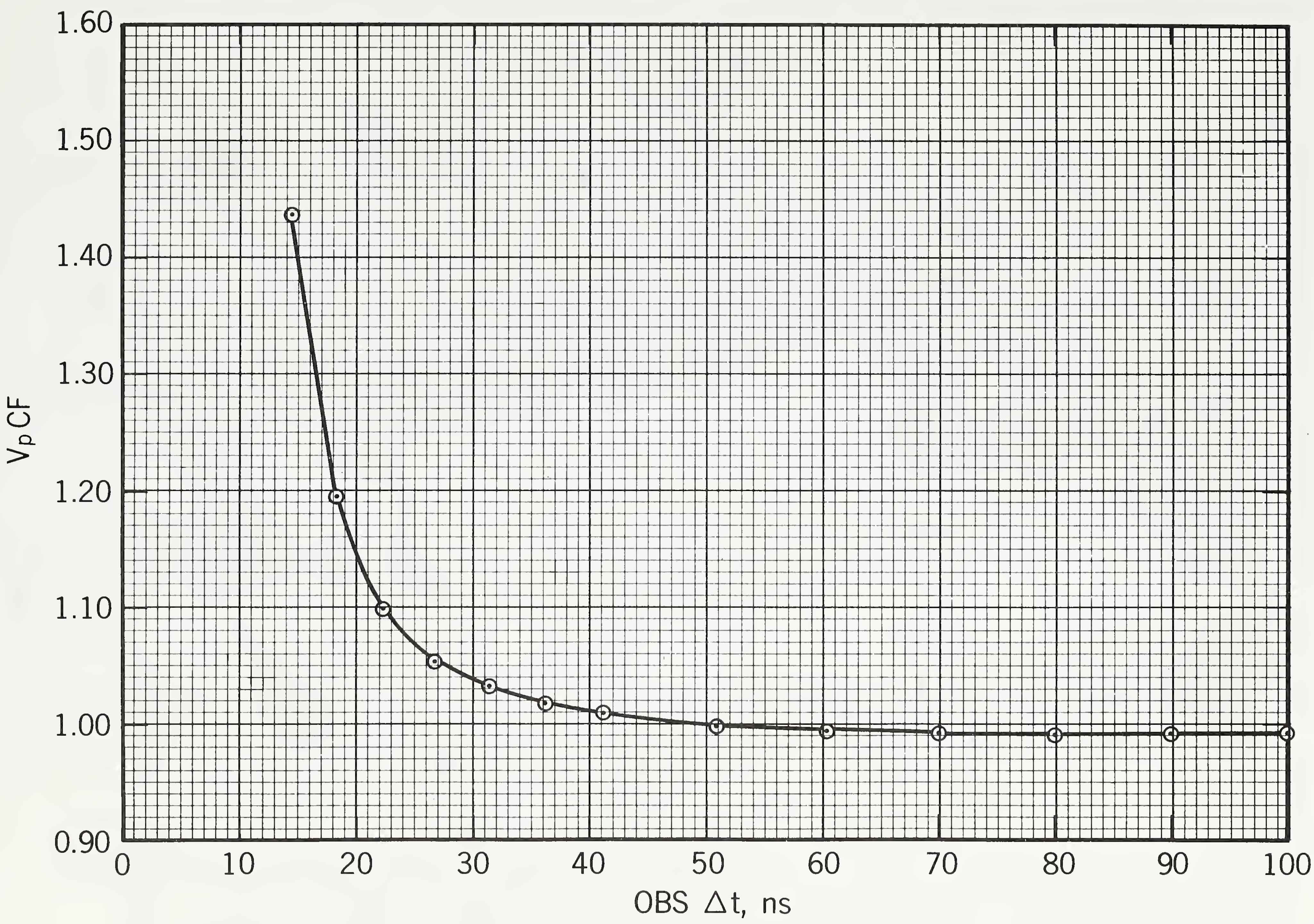

Figure 8. APD 723 - 20 dB - Filter - Run 20
Peak voltage correction factor (V_p CF) versus observed pulse duration (OBS Δt) for impulse response maximum of 59.9 mV.

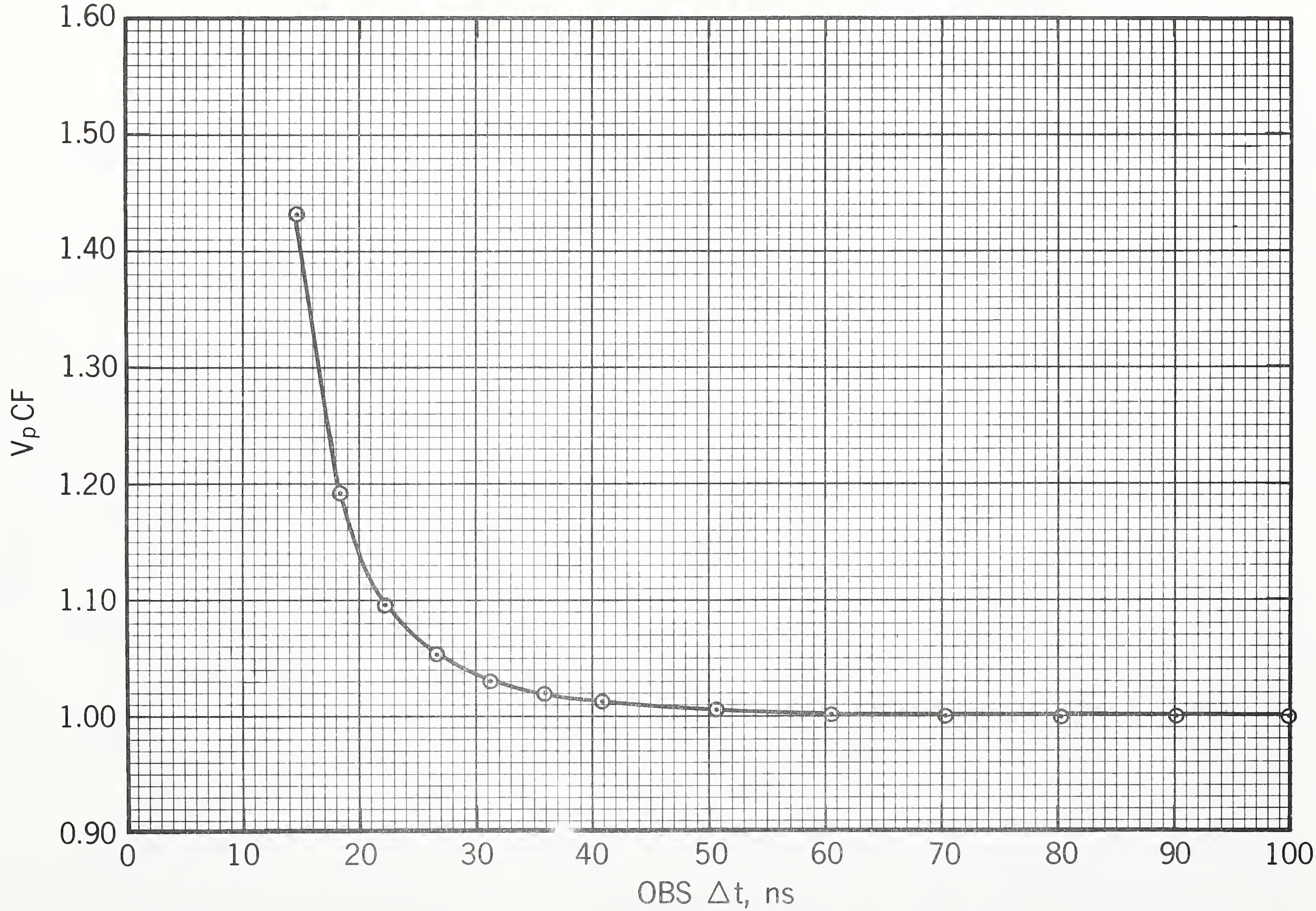

Figure 9. APD 723 - 40 dB - Filter - Run 21
Peak voltage correction factor (V_p CF) versus observed pulse duration (OBS Δt) for impulse response maximum of 248 mV.

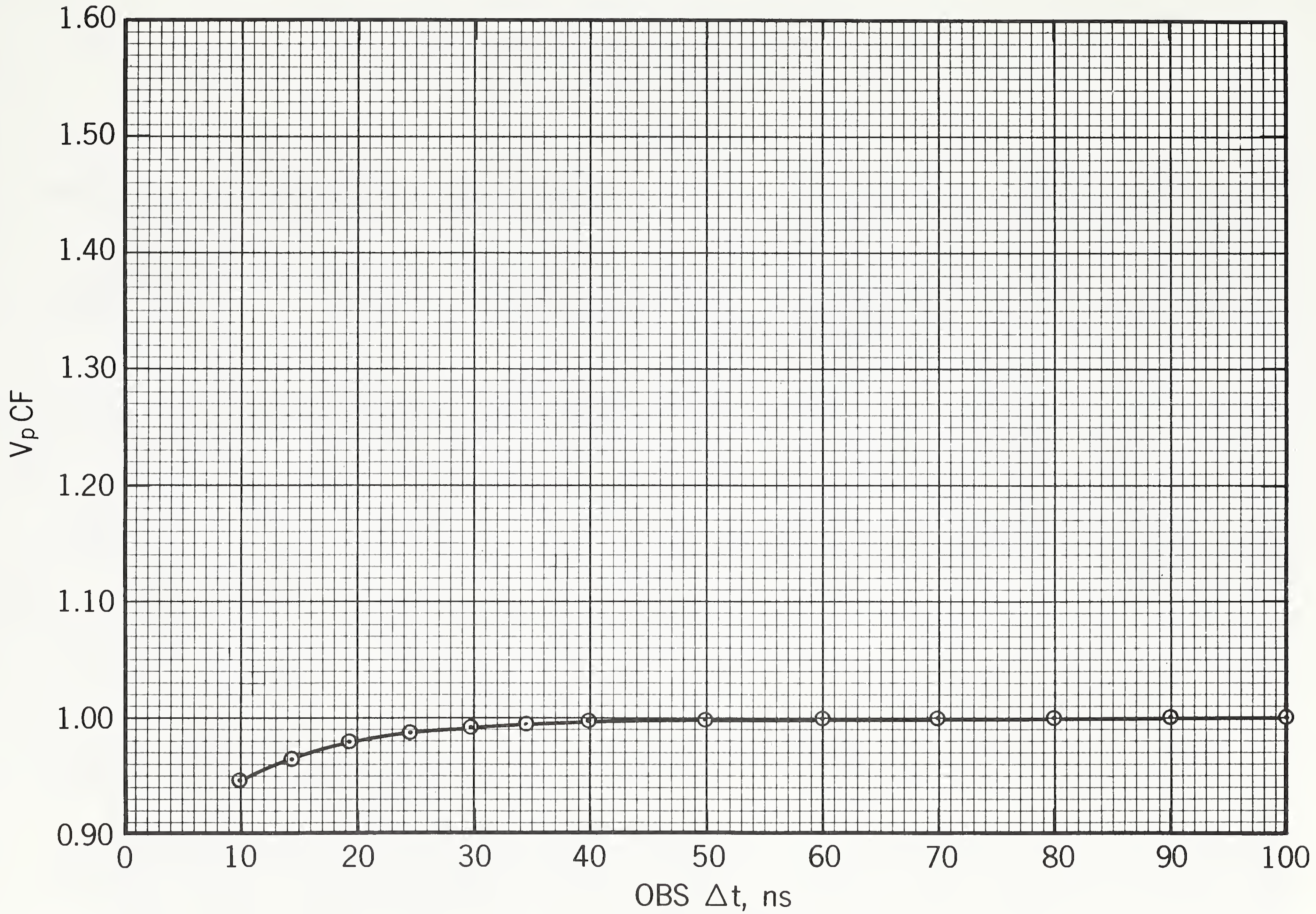

Figure 10. APD 725 - 0 dB - No Filter. (Average of runs 1 and 4). Average values of peak voltage correction factor (V_p CF) versus observed pulse duration (OBS Δt) in ns for impulse response maximum of 204 mV and 19.7 mV.

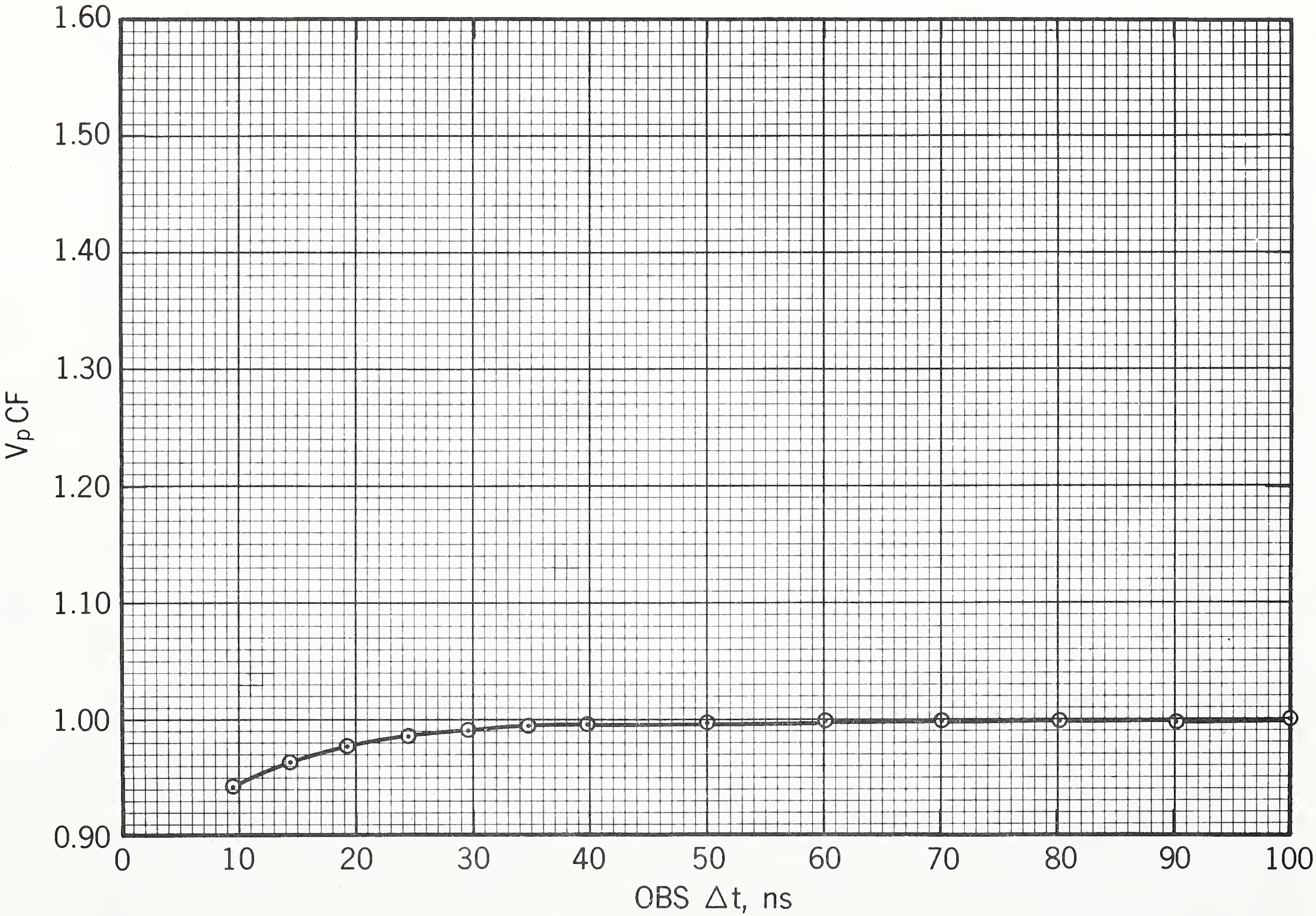

Figure 11. APD 725 - 20 dB - No Filter - Run 6
Peak voltage correction factor (V_p CF) versus observed pulse duration (OBS Δt) for impulse response maximum of 197 mV.

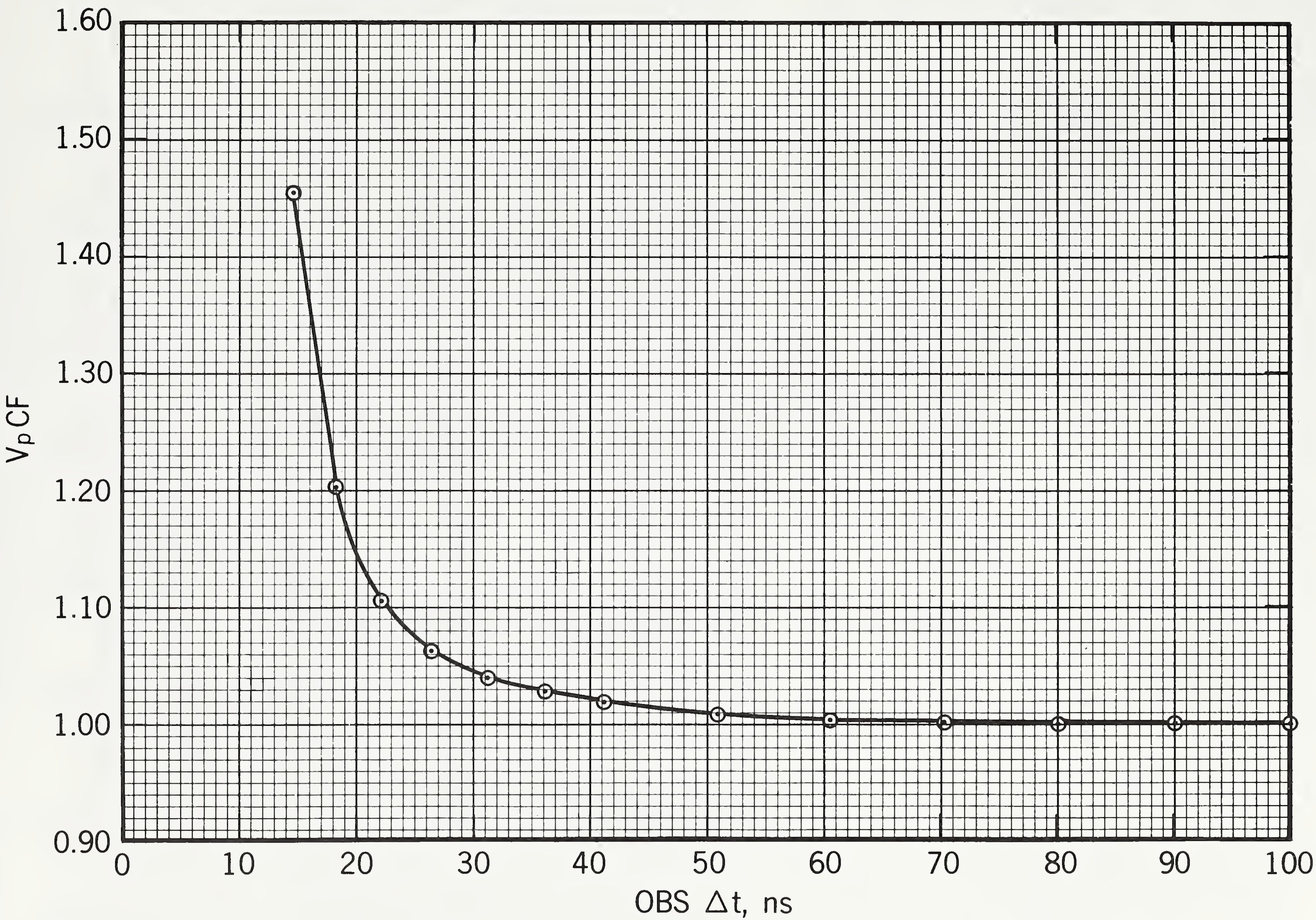

Figure 12. APD 725 - 20 dB - Filter - Run 15
Peak voltage correction factor (V_p CF) versus observed pulse duration (OBS Δt) for impulse response maximum of 51.1 mV.

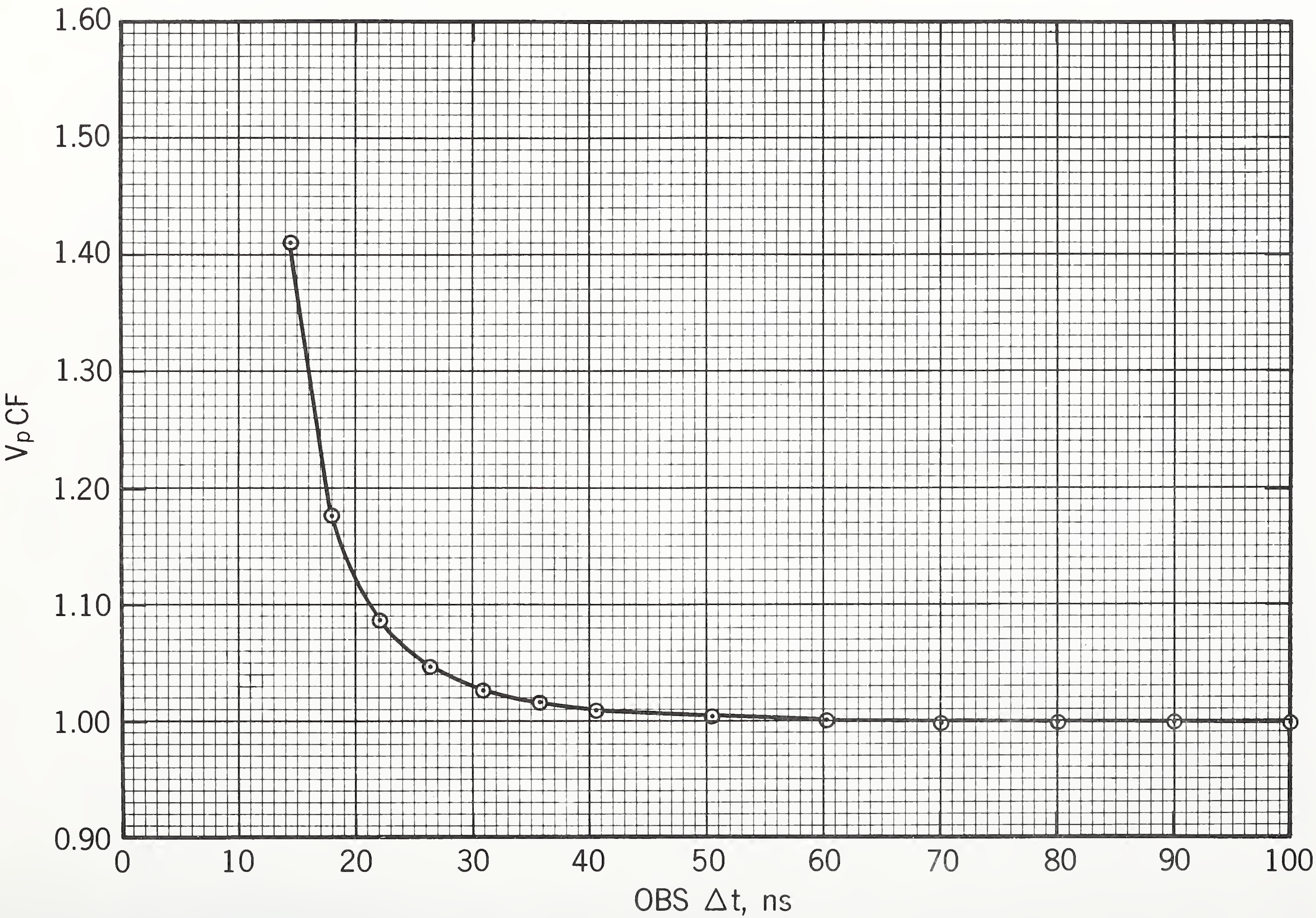

Figure 13. APD 725 - 40 dB - Filter - Run 14
Peak voltage correction factor (V_p CF) versus observed pulse duration (OBS Δt) for impulse response maximum of 238 mV.

NBS-114A (REV. 2-80)

U.S. DEPT. OF COMM. **BIBLIOGRAPHIC DATA SHEET** *(See instructions)*	1. PUBLICATION OR REPORT NO. NISTIR 89-3917	2. Performing Organ. Report No.	3. Publication Date August 1989

4. TITLE AND SUBTITLE

Improved Low-Level Silicon-Avalanche-Photodiode Transfer Standards at 1.064 Micrometers.

5. AUTHOR(S)

A.L. Rasmussen, P.A. Simpson, and A.A. Sanders

6. PERFORMING ORGANIZATION *(If joint or other than NBS, see instructions)*

National Institute of Standards and Technology
~~NATIONAL BUREAU OF STANDARDS~~
DEPARTMENT OF COMMERCE
WASHINGTON, D.C. 20234

7. Contract/Grant No.

8. Type of Report & Period Covered

9. SPONSORING ORGANIZATION NAME AND COMPLETE ADDRESS *(Street, City, State, ZIP)*

Aerospace Guidance and Metrology Center
Newark Air Force Station, Ohio

10. SUPPLEMENTARY NOTES

☐ Document describes a computer program; SF-185, FIPS Software Summary, is attached.

11. ABSTRACT *(A 200-word or less factual summary of most significant information. If document includes a significant bibliography or literature survey, mention it here)*

Three silicon-avalanche-photodiode (APD) transfer standards were calibrated from $\sim 10^{-8}$ to $\sim 10^{-5}$ W/cm^2 peak power density at approximately 10% uncertainty. These calibrations are for 1.064 μm wavelength pulses of 10 to 100 ns duration. For this calibration, an acousto-optically modulated laser beam generated alternately equal levels of pulsed power and cw power into a low-level beam splitter. The cw power measured by a transfer standard in the transmitted beam of the splitter was used to determine the pulsed power into the APD transfer standard in one of the low-level reflected beams of the splitter. The APD detector had about a 1 cm^2 aperture and a 3.8 cm focal length lens in front of it. Lens, window, and detector surfaces had narrow-band antireflection coatings. The commercial detector package is a temperature compensated, infrared-enhanced APD preamplifier module. To increase the sensitivity, one or two 20 dB, 500 MHz bandwidth amplifiers followed the preamplifier. With very low pulsed power, a 30 MHz low-pass filter with Gaussian roll-off was attached to the amplifier output to reduce the noise. A transient digitizer recorded the impulse responses of the APD detectors at 1.064 μm. These data were read into computer programs that convolved the unit-area impulse response with unit-height Gaussian pulses. From these data, correction factors of the pulse peak for observed pulse durations from 10 to 100 ns were determined. Instructions, calibrations, error budgets, and system descriptions are included.

12. KEY WORDS *(Six to twelve entries; alphabetical order; capitalize only proper names; and separate key words by semicolons)*

detector impulse response; laser detectors; laser pulse standards; low-level pulse detectors; pulse power measurements; YAG laser pulse calibrations

13. AVAILABILITY

☒ Unlimited
☐ For Official Distribution. Do Not Release to NTIS
☐ Order From Superintendent of Documents, U.S. Government Printing Office, Washington, D.C. 20402.
☒ Order From National Technical Information Service (NTIS), Springfield, VA. 22161

14. NO. OF PRINTED PAGES

44

15. Price